Palaeogeography, Palaeoclimatology, Palaeoecology 567 (2021) 110243

Contents lists available at ScienceDirect

Palaeogeography, Palaeoclimatology, Palaeoecology

journal homepage: www.elsevier.com/locate/palaeo

An Upper Pleistocene macroflora indicates warm and dry climate during an interglacial in central Brazil

Gabriela Luiza Pereira Pires Follador [a,*], Raquel Franco Cassino [a], Angélica F. Drummond C. Varajão [a], Jonathas S. Bittencourt [b]

[a] Departamento de Geologia, Universidade Federal de Ouro Preto, Brazil
[b] Laboratório de Paleontologia e Macroevolução (CPMTC), Departamento de Geologia, Instituto de Geociências, Universidade Federal de Minas Gerais, Brazil

ARTICLE INFO

Keywords:
Cerrado
Pleistocene
Leaf Margin analysis
Leaf Area analysis
South American summer monsoon
Paleoclimate

ABSTRACT

This study is the first report of the fossil macroflora of the Paleolagoa Seca, an Upper Quaternary fossil locality of lacustrine origin in central Brazil. Here we present an analysis of well-preserved fossil leaves collected from an argillite level dated at ca. 43,000 cal yr BP and discuss the paleoclimatic implications of this record. We reconstructed paleotemperature and paleoprecipitation using Leaf Margin Analysis (LMA) and Leaf Area Analysis (LAA), respectively, and used mineralogical (XRD and IR) and palynological analyses of the fossiliferous level to assess a complete picture of the past landscape. To test the ability of LMA and LAA models available for Southern Hemisphere to correctly predict Mean Annual Temperature (MAT) and Mean Annual Precipitation (MAP) for the Paleolagoa Seca, we applied several calibration models to the leaf dataset of a modern Cerrado forest and then compared predictions with modern climate data. Six LMA calibration models presented consistent MAT results and all four LAA calibration models provided satisfactory estimations of the modern MAP. The botanical identification of the fossil leaves and the pollen record indicated a mosaic of open savanna, dry forests and gallery forest around the Paleolagoa Seca. The reconstructed MAP for the Paleolagoa Seca ranged between 647 and 948 mm depending on the LAA equation, which is at least 500 mm lower than the current MAP. The reconstructed Mean Annual Temperature (MAT) ranged between 22.6 and 26.3 °C, indicating a higher-than-present MAT, which we relate to a combination of high summer insolation and low humidity. Comparison with other local fossil macrofloras, including from nearby localities, and with other paleoclimatic records suggests that the observed dry conditions at Paleolagoa Seca were related to interhemispheric climate forcing and to a weakening of the South American Summer Monsoon (SASM).

1. Introduction

The Paleolagoa Seca sedimentary succession is a lacustrine deposit of Pleistocene age located in the south of the Cerrado biome, in central Brazil (Fig. 1). This deposit contains a well-preserved macroflora that constitutes an unexplored record of the paleoflora and paleoclimate of the Pleistocene of the Cerrado.

The Cerrado is a Neotropical savanna that extends from 5° to 24°S latitude, covering the central region of Brazil (Fig. 1A). The vegetation of the Cerrado is highly diverse and forms several types of physiognomies categorized as forest formations (Riparian, Gallery and Dry Forests, and Savanna Woodlands (*Cerradão*)); savanna formations (*Cerrado senso strictu*) and grasslands and shrubby-grasslands (Ribeiro and Walter, 2008). This biome is characterized by a highly seasonal climate, with almost all of the rainfall concentrated in the austral summer and a dry winter season (Oliveira Filho and Ratter, 2002). The summer precipitation is related to the activity of the South American Summer Monsoon (SASM) system (Silva and Kousky, 2012), of which the main features are the Intertropical Convergence Zone (ITCZ) and the South Atlantic Convergence Zone (SACZ). This climatic system is known to have varied during the Pleistocene in response to interhemispheric forcing (Kanner et al., 2012; Mosblech et al., 2012), but the regional extent of this variability and its impact on the vegetation of central Brazil is still poorly known.

The Paleolagoa Seca deposit and its sedimentary rocks, pollen and fossil leaves provide a comprehensive record of the landscape at a specific timeframe of Late Pleistocene that illustrates the impact of climate variability on southern Cerrado. In this study, we present a floristic

* Corresponding author at: Departmento de Geologia, Universidade Federal de Ouro Preto, Campus Morro do Cruzeiro, Ouro Preto CEP 35400-000, MG, Brazil.
E-mail addresses: gabriela@pires.bio.br (G.L.P.P. Follador), raquelcassino@ufop.edu.br (R.F. Cassino).

https://doi.org/10.1016/j.palaeo.2021.110243
Received 4 November 2020; Received in revised form 13 January 2021; Accepted 14 January 2021
Available online 19 January 2021

reconstruction for the Paleolagoa Seca site, based on the botanical identification of fossil leaves, pollen analysis and a paleoclimate reconstruction (paleotemperature and paleoprecipitation), based on Leaf Margin Analysis (LMA) and Leaf Area Analysis (LAA). We compare our results with other paleofloristic and paleoclimatic data in order to discuss the interaction between the Cerrado vegetation, the lacustrine deposition at the site and the variability of the SASM.

2. Study site

2.1. Geological setting

The Paleolagoa Seca fossil locality consists of a deposit of lacustrine sedimentary rocks, around 50 m-thick, that crops out in the eastern area of a phosphate mine. This phosphate mine is located in the central area of an ultramafic-alkaline-carbonatite complex, named Catalão I, within the municipality of Catalão, State of Goiás (Fig. 1). The Catalão I complex forms a subcircular plateau (carbonatite dome) supported by embedded quartzite rocks. Near the Paleolagoa Seca, on the same carbonatite dome, there is another succession of lacustrine sedimentary rocks, known as Paleolago Cemitério (referred to as Cemitério Paleolake by Machado et al., 2013, 2014) (Fig. 1E). The Catalão I complex is part of a group of six Cretaceous magmatic provinces, also including Catalão II, Serra Negra, Salitre, (Fig. 1B), Araxá and Tapira domes (de Toledo, 1999) that occur along deep faults at the edges of the Paraná Basin (Ribeiro et al., 2001).

Ribeiro et al. (2001) proposed two hypotheses to explain the development of the Paleolagoa Seca in the Catalão I dome. The first hypothesis involves the formation of a depression resulting from leaching of carbonates from carbonatites and underlying phoscoritos, eventually forming caves and dolines or reducing the original rock volume. In the second hypothesis, the depression resulted from small-scale collapses related to the cooling and solidification of the central carbonate stocks of the dome. The presence of quartzite and carbonatite fragments in the basal conglomerates of Paleolagoa Seca attests that at the beginning of the lacustrine deposition the complex had already been exposed at the surface through erosive processes, thus supporting the first hypothesis.

The Paleolagoa Seca deposit consists mainly of a sequence of argillites and contains a level of grey argillite hosting abundant fossil leaves that constitutes the main focus of this study. The nearby-located

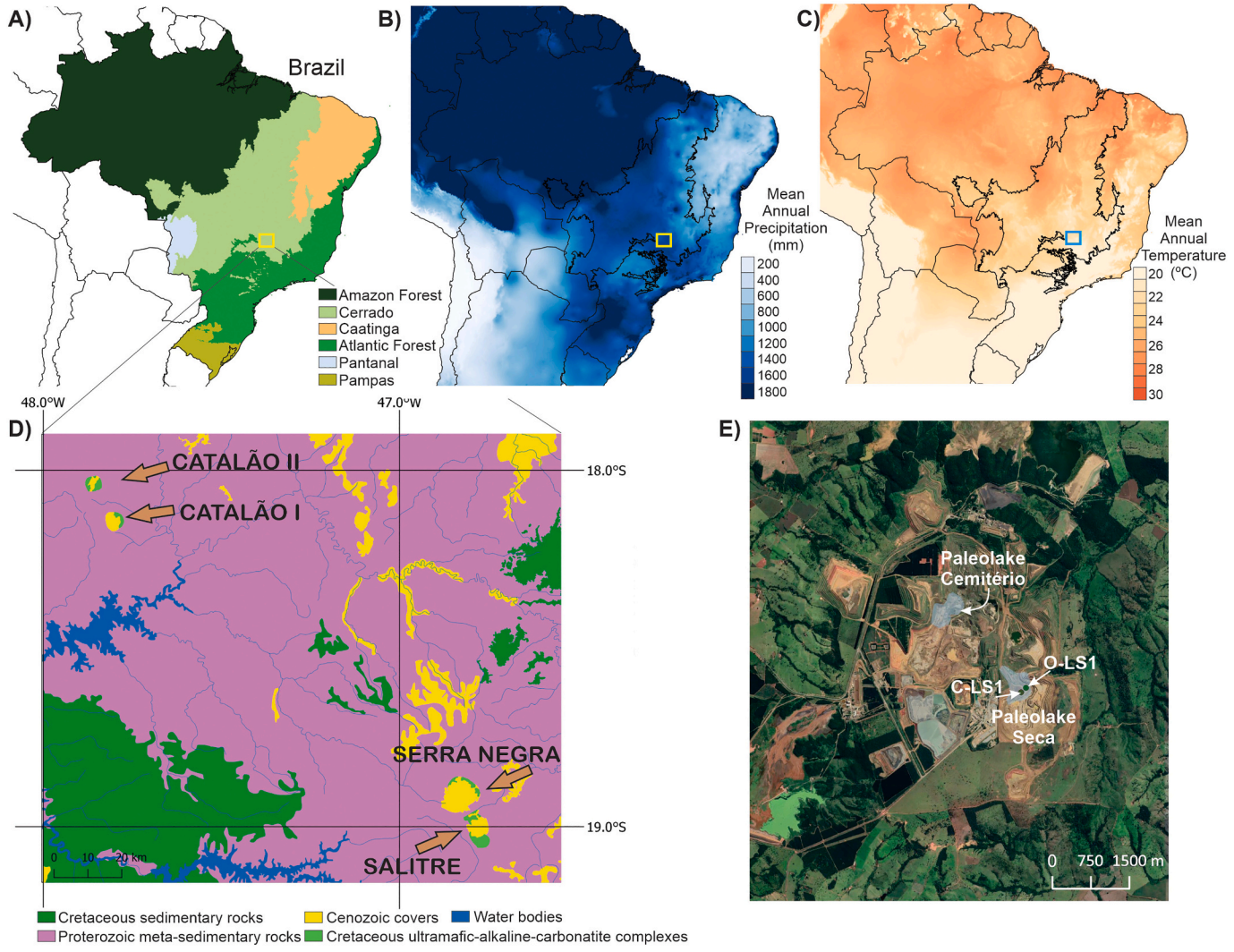

Fig. 1. Location of the Paleolagoa Seca. A) Map of South America showing the distribution of Brazilian Biomes (IBGE, 2004) and the location of the study area (yellow rectangle) B) Map of Annual Precipitation (mm) in South America (Fick and Hijmans, 2017) C) Map of Mean Annual Temperature (°C) of South America (Fick and Hijmans, 2017) D) Geological map of the Paleolagoa Seca region (modified from CPRM, 2005) showing the location of magmatic domes Catalão I and II, Serra Negra and Salitre E) Satellite image (Google Earth) of phosphate mines in the Catalão Magmatic Dome I showing the location of the Paleolagoa Seca and Paleolago Cemitério, and of the core (C-LS1) and outcrop (O-LS1) presented in this study. (For interpretation of the references to colour in this figure legend, the reader is referred to the web version of this article.)

Paleolago Cemitério also contains rich paleofloras and sponge spicule deposits previously studied by Cardoso and Iannuzzi (2006), Silva (2013) and Machado et al. (2013, 2014).

2.2. Modern vegetation and climate

The Catalão I complex is located in the southern region of the Cerrado biome, close to the transition with the Atlantic Forest (Fig. 1A). A land cover mapping of the municipality of Catalão performed by da Silva and Rosa (2019) showed that today agriculture and pasture occupy most of the municipality, covering 31% and 28% of its rural area, respectively. As for native vegetation cover, around 20% is occupied by open formations such as sparse savanna (*Cerrado ralo*), shrubby grasslands (*Campo Sujo*) or montane savanna (*Campo Rupestre*) and around 11% is occupied by riparian forests, gallery forests or palm swamps. Savanna woodlands (*Cerradão*) and dry forests (*Mata Seca*) occupy respectively 1.5% and 0.3% of the municipality area (da Silva and Rosa, 2019). A survey of the woody flora of a shrubby grassland in Catalão performed by Ferreira and Cardoso (2013) indicated Fabaceae, Asteraceae, Vochysiaceae, Erythroxylaceae and Dilleniaceae as families with the highest Importance Value index and *Piptocarpha rotundifolia*, *Erythroxylum tortuosum*, *Qualea grandiflora*, *Connarus suberosus*, *Roupala montana*, *Curatella americana*, *Davilla elliptica*, *Stryphnodendron polyphyllum*, *Diospyros hispida* and *Stryphnodendron adstringens* as the most important species. Another study (Ferreira and Moreno, 2010) presented a floristic survey including areas of open savanna, montane savanna, savanna woodland and gallery forest close to the urban area of Catalão. This study indicated Fabaceae, Myrtaceae and Vochysiaceae as the most diverse families and *Pterodon pubescens*, *Sclerolobium paniculatum*, *Qualea grandiflora*, *Eugenia dysenterica*, *Plathymenia reticulata*, *Xylopia aromatica*, *Byrsonima coccolobifolia*, *Neea theifera*, *Myrcia variabilis* as species with highest importance values.

According to the Köppen classification, the climate of the region is of the Aw type, i.e. tropical with rainy summers and dry winters (Alvares et al., 2013). The dry season extends from April to September and the rainy season from October to March. The mean annual temperature of Catalão, considering available data for the period between 1961 and 2019, is 22.6 °C and the mean annual precipitation for the same period is 1434 mm (data from the Catalão meteorological station, available at the BDMEP/INMET; http://www.inmet.gov.br).

3. Materials and methods

3.1. Sampling and dating methods

The study of the Paleolagoa Seca fossil record was based on the analysis of a core and a surface outcrop. A ~ 37 m-thick core, C-LS1, was collected at 18° 8′30″S, 47° 47′30″W (Fig. 1D), with an Atlas Copco model CS-14 probe in 2013, as a result of the cooperation between the Federal University of Minas Gerais (UFMG) and the company *Vale Fertilizantes*, that was then in charge of the exploration of the Catalão phosphate mine. The description of the core lithology was performed during the coring process and selected samples were transported and stored at the *Laboratório de Paleontologia e Macroevolução* - CPMTC/IGC/UFMG. Three samples (samples C-LS-27.30, C-LS-26.40 and C-LS-25.90) from the fossiliferous level and adjacent layers were sent for radiocarbon dating by Accelerator Mass Spectrometry (AMS) at Beta Analytic Laboratory (Miami, US).

A systematic sampling of the fossil leaves was performed in the outcrop (O-LS1) of the Paleolagoa Seca sedimentary sequence. The fossils are housed at the *Laboratório de Paleontologia e Macroevolução* - CPMTC/IGC/UFMG. Samples for mineralogical analysis were also collected from the fossiliferous and adjacent levels.

3.2. Mineralogical analysis

Eight C-LS1 samples (C-LS1–12.5, C-LS1–17.5, C-LS1–20, C-LS1–26.40, C-LS1–27.30, C-LS1–28, C-LS1–32 and C-LS1–37) and six O-LS1 samples (Fig. 2) were used for mineralogical analysis by X-ray diffraction (XRD). The analyses were performed at the Geology Department of the Federal University of Ouro Preto (UFOP) using an Empyrean Panalytical diffractometer (CuKα, 45 KV and 40 mA) and at the Manuel Teixeira da Costa Research Center (CPMTC-IGC) of the Federal University of Minas Gerais (UFMG) using a Panalytical X'Pert PRO diffraction instrument (CuKα, 45 KV and 40 mA). After drying at room temperature, the samples were gently powdered in agate mortar and the clay fraction (<2 μm) was separated by sedimentation using the centrifuge SORVAL LegendT. For the bulk random samples, XRD patterns were obtained in the range of 2°–70° 2θ, step of 0.02° 2θ and count of 10″/step. For the clay fraction, oriented preparations were made, air dried, ethylene glycol solvated and heated to 550 °C. XRD patterns were acquired using the same step and counting time but in the range of 2°–35° 2θ. For the clay fraction of sample LS-26.40, a saturation with K^{1+} and Mg^{2+} and a new scan were performed in order to obtain a better identification of clay minerals. XRD patterns were interpreted using High Score X'Pert Plus software and known patterns from the literature (Brindley and Brown, 1980).

The infrared spectroscopy (IR) was used to complement the XRD analyses. It was performed in the IC2MP Institute, University of Poitiers, using a Fourrier transform spectrometer (Thermo Nicolet, Nexus 5700 series) for analyses of the clay fractions. Pressed discs were made with 1 mg of sample and 150 mg of KBr, which were analyzed with natural moisture and then dehydrated at 120 °C overnight to remove absorbed water. The mid-infrared spectra (4000–400 cm^{-1}) were obtained using source of white light, beamsplitter KBr, resolution of 4 cm^{-1}, optical velocity of 0.4747 cm s^{-1} and 100 scans.

3.3. Macroflora and pollen analyses

A total of 171 fossil samples recovered from the Paleolagoa Seca were mechanically prepared (Feldman et al., 1989) with brushes, tips and pneumatic pens. The specimens were classified in morphotypes based on the Manual of Leaf Architecture (Ash et al., 1999; Ellis et al., 2009). For each specimen, a complete morphological description was performed, including laminar size, laminar L:W ratio, medial symmetry, base symmetry, margin type, base angle, base shape, apex angle, apex shape, primary vein framework, naked basal veins, number of basal veins, agrophic veins, major secondary vein framework, major secondary spacing, variation of major secondary angle to midvein and major secondary attachment to midvein (Ellis et al., 2009). Morphotypes were assigned to modern taxa based on the comparison with specialized bibliography (Brotto et al., 2013; Dutra et al., 2012; Margalho, 2009; Martins and Pirani, 2010; de Mattos et al., 2018; de Oliveira et al., 2011; Santos-Silva et al., 2015; Silva, 2013; de Sousa et al., 2018) and with online herbarium collections (speciesLink Network; http://splink.org.br).

The sample C-LS- 26.40 from the fossiliferous level (Fig. 2) was prepared for pollen analysis in order to compare the macro and microfloras preserved in this unit. The sample was prepared using standard laboratory techniques (Faegri and Iversen, 1989) including treatments with HF-40%, HCL-30%, KOH-10% and acetolysis. After treatment, three slides were mounted with Entellan. A total of 300 terrestrial pollen grains were counted.

3.4. Paleoclimate reconstruction

Paleotemperature and paleoprecipitation were reconstructed using Leaf Margin Analysis (LMA) and Leaf Area Analysis (LAA), respectively. In this study, these univariate methods were preferred over the multivariate Climate-Leaf Analysis Multivariate Program (CLAMP; Wolfe, 1995) because of the uncertainty in the determination of some leaf

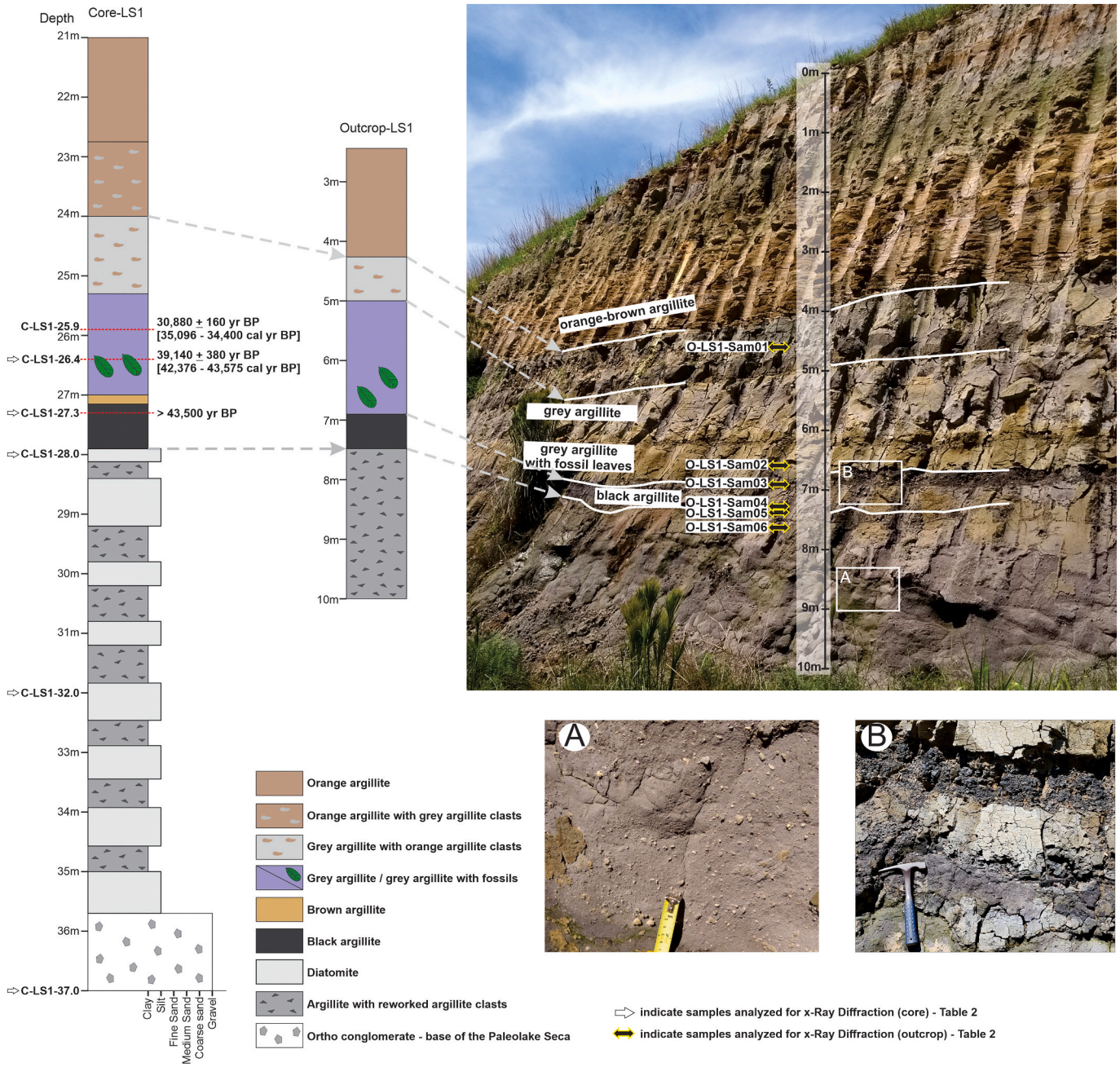

Fig. 2. Lithostratigraphic profile of Paleolagoa Seca core (C-LS1) and outcrop (O-LS1). A) Argillite with reworked argillite clasts level. B) Black argillite level.

characters required by CLAMP in some fossil specimens. Nonetheless, LMA and LAA have been reported to be as accurate as CLAMP analyses (Peppe et al., 2018).

LMA is the most widely used tool to reconstruct Cenozoic continental paleotemperatures from fossil floras because this method is independent of the taxonomic determination of each fossil leaf and uses one single morphological character (Wolfe, 1995; Wilf, 1997; Peppe et al., 2018). LMA is an univariate linear regression technique that relates the proportion of woody dicot species with entire margins (pE) and the mean annual temperature (MAT) (Wolfe, 1979; Wing and Greenwood, 1993):

$$LMAT = c \times pE + \alpha \quad (1)$$

where *LMAT* is the value in °C of the *Leaf-Estimated Mean Annual Temperature* and *pE* is the proportion of entire-margined leaves; the constant *c* and the intercept α are specific to regional models because the pE-MAT relationship is not globally uniform (Kennedy et al., 2014).

Several models relating pE and MAT have been proposed from leaf datasets representing floras from different ecoregions (reviewed in Peppe et al., 2018). Significant differences that are found in the pE-MAT relationship between Southern and Northern hemispheres floras (Kowalski, 2002; Kennedy et al., 2014; Peppe et al., 2018) are likely due to both phylogenetic and ecological factors (Peppe et al., 2018). In summary, Southern Hemisphere floras have a higher proportion of entire-margined leaves than those of Northern Hemisphere for any given MAT (Kennedy et al., 2014). In this study, we initially used ten equations proposed in the literature that include data from South America (Table 1).

The uncertainty of LMAT estimations was calculated with the formula proposed by Miller et al. (2006):

Table 1
Equations for MAT calculation from models that include South American sites.

Model	LMAT Equation	SE	n	r^2	Reference
North, Central, South America	(1) 28.6pE + 2.240	2	9	0.94	Wilf (1997)
South America	(2) 31.6pE − 0.059	1.6	14	0.89	Gregory-Wodzicki (2000)
Tropical South America	(3) 38.5pE − 10.24	±3.4	30	0,47	Kowalski (2002)
South America (isotherm)	(4) 38.25pE − 10.9	–	16	0.733	Aizen and Ezcurra (2008)
South America (cell)	(5) 42.36pE − 11.37	–	16	0.535	Aizen and Ezcurra (2008)
South America	(6) 26.03pE − 1.31	2.8	51	0.82	Hinojosa et al. (2011)
South America	(7) 43.96pE − 8.3637	1.73	14	0.9256	Kennedy et al. (2014)
Southern Hemisphere	(8) 25.7pE − 1.8412	4.83	90	0.40406	Kennedy et al. (2014)
Oceania, Japan, North America, South America, Southern Africa	(9) 20.39pE + 3.6562	3.97	239	0.5733	Kennedy et al. (2014)
Global	(10) 19.4pE + 5.884	4.54	1488	0.42	Peppe et al. (2018)

LMAT: Leaf Margin Annual Temperature; pE: proportion of entire-margined species; SE = Standard Error; n = number of sites in the sampled dataset; r^2 = coefficient of determination.

$$\sigma[LMAT] = c\sqrt{1 + \varphi(n-1)(P(1-P))\frac{P(1-P)}{n}} \quad (2)$$

where $\sigma[LMAT]$ is the standard deviation in °C of the estimated temperature; c is the slope of the equation, P is the proportion of species with entire margins and φ, the overdispersion factor for P (Miller et al., 2006). According to Peppe et al. (2018), this formula provides the best estimation of *LMAT* precision since it incorporates the uncertainty associated with the estimation of the entire-margined leaves proportion in the flora.

Leaf Area Analysis (LAA) is also an univariate linear regression technique. It was originally proposed by Wilf et al. (1998) who used the correlation between the mean natural logarithm of the leaf area (MlnA) and the natural logarithm of MAP (lnMAP) of 50 sites from North, Central and South America and Africa to develop a predictive equation for MAP:

$$ln(MAP) = c^{*}MlnA + \alpha \quad (3)$$

where c and α are also regionally defined constants (Table 2), and ***MlnA*** is calculated based on Raunkiaer-Webb size categories and the proportion of species in each category:

$$MlnA = \sum a_i p_i \quad (4)$$

where *ai* is the mean of the natural logarithm area of the leaf size categories (Leptophyll - 2.12, Nanophyll - 4.32, Microphyll - 6.51, Notophyll - 8.01, Mesophyll - 9.11, Macrophyll - 10.9 and Megaphyll - 13.1) and *pi* is the proportion of species in each category.

Specific calibrations for tropical Southern Hemisphere were initially developed with datasets from Africa (Jacobs, 1999) and Bolivia (Gregory-Wodzicki, 2000). Jacobs and Herendeen (2004) then used both African and Bolivian datasets to produce an equation for tropical Southern Hemisphere (Eq. (2), Table 2) and, additionally, documented a strong relationship between mean leaf area and the precipitation of the wettest months (months with ≥50 mm) for this tropical dataset. This relationship was used to develop an equation to calculate the "wet month precipitation" (Wet-m-P, Eq. (3), Table 2). By calculating both MAP and Wet-m-P, it is possible to provide an estimation of the rainfall distribution between the rainy and dry seasons, an important parameter for deciphering past climate dynamics (Jacobs and Herendeen, 2004). In addition to these two equations, and the original equation from Wilf et al. (1998), we also used another equation proposed by Jacobs and Herendeen (2004), and a global equation proposed by Peppe et al. (2018) (Table 2).

Table 2
Equations used for MAP calculation.

Model	Equation ln(MAP) ($c \times MlnA + \alpha$)	SE	N	R^2	Reference
North and South America and Africa	(1) 0.548MlnA + 0.768	0.359	50	0.760	Wilf et al. (1998)
Tropical Africa and Bolivia	(2) 0.309MlnA + 2.566		42	0.734	Jacobs and Herendeen (2004)
	(3) ln(Wet-m-P) = 0.367MlnA + 2.07		42	0.178	Jacobs and Herendeen (2004)
North and South America and Africa	(4) 0.354MlnA + 2.167		79	0.709	Jacobs and Herendeen (2004)
Global	(5) 0.346MlnA + 2.404	0.93	184	0.41	Peppe et al. (2018)

In addition to the Paleolagoa Seca, we also applied LMA and LAA to the three paleofloras of the Paleolago Cemitério using data presented by Silva (2013) who studied the fossil leaves of three fossil levels of the Paleolago Cemitério.

To evaluate if LMA and LAA equations presented in Tables 1 and 2 could accurately estimate the paleotemperature and paleoprecipitation of the paleolakes Seca and Cemitério, we previously tested the equations with a modern forest locality with similar geographical conditions and compared MAT and MAP predictions with data from instrumental records. The chosen forest locality was the Panga Ecological Station, located at Uberlândia (Brazil), around 80 km south of Catalão, which was surveyed by Schiavini (1990) and Lopes and Schiavini (2007). The specimens collected in this survey are available in herbarium collections from the Herbarium Uberlandense (HUFU) and the Herbário da Universidade Estadual de Campinas (UEC) and can be consulted online (reflora.cria.org.br/exsiccatae). From the 99 dicot species listed for the Panga Forest, 82 were available in the herbarium collections and were used in this study. The area of at least two leaves from each species were measured with the INCT Exsiccatae Viewer that provides high-resolution images of exsiccates. Although the use of herbarium specimens is not ideal since the entire range of leaf size for each species may not be represented, herbarium collections have been effectively used in leaf-based climate reconstruction studies, including some of the studies that generated the calibrations used here (e.g. Jacobs, 1999; Hinojosa et al., 2011). Climatic data (MAT and MAP) for the Panga Forest were obtained from the closest INMET (http://www.inmet.gov.br) meteorological station for the period between 1981 and 1990, the ten years preceding the floristic survey (Schiavini, 1990) from which the leaf physiognomic characters were obtained.

4. Results

4.1. Lithology and chronology of the Paleolagoa Seca

The bottom of the outcrop O-LS1 sequence is composed of a 2.5 m-thick argillite layer with abundant reworked argillite clasts, followed upwards by a layer of black argillite (Fig. 2). This black argillite layer corresponds to the level between 28 and 27.15 m of the core C-LS1. Below this layer, the C-LS1 sequence is characterized by interleaving argillite with argillite clasts and diatomite layers.

Above the black argillite layer, both O-LS1 and C-LS1 present a ~1.5 m-thick layer of grey argillite with abundant fossil leaves. The fossils are concentrated in the level situated just above the black argillite, corresponding to the layer between 26.4 m and 26.7 m of C-LS1 (Fig. 2). From the top of the grey argillite layer upwards, both C-LS1 and O-LS1 showed the predominance of grey argillite with abundant orange clay clasts. The orange-brown argillite then dominates the profiles up to the top of the section (Fig. 2).

The ^{14}C age yielded by sample C-LS1–26.4 from the grey argillite fossiliferous level situates the deposition of this level around 42,376 to 43,575 cal yr BP (Table 3). The sample from the black argillite (C-LS1–27.3) was beyond the laboratory dating range and did not produce an age. Sample C-LS1–25.9 from the grey argillite above the fossiliferous level yielded an age of 34,400 to 35,096 cal yr BP (Table 3).

The XRD analyses (Table 4) revealed a mineralogical association composed by kaolinite, quartz, hydrated phosphates (crandallite, goyazite or plumbogummite group, wavellite and vivianite) and anatase. In addition to these minerals, samples from the core C-LS1 also indicated the presence of carbonates (dolomite, dawsonite and huntite) hematite, magnetite and goethite. Jarosite, an iron hydrosulphate, occurred only in the outcrop sample from the fossiliferous level.

The IR spectra of the clay samples showed only the three stretching vibrations of Kaolinite at 3654, 3698, 3620 cm^{-1} and the bending band at 915 cm^{-1} (Farmer, 1974). The spectra also showed the presence of organic matter, represented by the bands around 1400, 1635, 2340, 2927 and 3400 cm^{-1}, and quartz around 790 cm^{-1}.

4.2. Paleolagoa Seca macroflora and pollen record

The Paleolagoa Seca fossils are preserved by carbonization or, more rarely, by impressions (7% of the fossils). Nineteen morphotypes related to dicot taxa were described from the macroflora (Table 5, Figs. 3, 4); additionally, fern fronds related to the species *Pteridium arachnoideum* were also found. Eighteen out of nineteen morphotypes had entire margins and only one was toothed, reaching a proportion of entire-margined species of 95%. Regarding the size, 68% of the leaves were microphyll, 21% nanophyll and 11% notophyll (Table 5). The diversity of morphotypes in the flora is at the lowest limit but still in the range of the required number for paleoclimate analysis (Peppe et al., 2018).

Seventeen of the nineteen morphotypes could be assigned to modern taxa (Table 5). The following families were represented in the macroflora: Aquifoliaceae (1 taxon), Combretaceae (1 taxon), Fabaceae (4 taxa), Lauraceae (2 taxa), Malvaceae (1 taxon), Melastomataceae (1 taxon), Moraceae (2 taxa), Myristicaceae (1 taxon), Myrtaceae (1 taxon), Rubiaceae (1 taxon), Sapindaceae (1 taxon) and Opiliaceae (1 taxon).

The pollen analysis of the layer containing the fossils revealed a high frequency (54%) of herbaceous pollen (mainly Poaceae and Asteraceae; Fig. 4) and the presence of herbaceous swamp indicators (Cyperaceae, *Xyris*, *Ludwigia*); algae zygospores, however, were absent. Melastomataceae, Myrtaceae and *Symplocos* were the most abundant arboreal pollen (Fig. 4).

4.3. Leaf Margin and Leaf Area analyses

4.3.1. Modern forest – Panga Ecological Station

The leaf physiognomy analysis of the modern riparian forest of the Panga Ecological Station revealed a percentage of entire-margined species equal to 89%. The size categories were distributed as follows: nanophyll – 2.4%; microphyll – 39%; notophyll – 39%; mesophyll – 15%; and macrophyll – 1.2%.

The actual MAT of the locality calculated from meteorological data was 22 °C. Three LMAT models provided accurate predictions for the Panga Ecological Station, within the error range: the South American model based on isotherms from Aizen and Ezcurra (2008) and two equations from Kennedy et al. (2014) (Table 6). Three other equations provided LMAT predictions close to the real MAT, overestimated by only 1 to 2 °C: the one from Kowalski (2002), the one from Hinojosa et al. (2011) and the global equation from Peppe et al. (2018); the other four equations overestimated MAT by more than 4 °C (Table 6).

The modern MAP at the Panga Ecological Station calculated from meteorological data was 1456 mm. The reconstruction of MAP from LAA resulted in relatively accurate estimations. The equations from Wilf et al. (1998) and from the African-Bolivian dataset of Jacobs and Herendeen (2004) predicted MAPs around 100 mm lower than the actual MAP (Table 6). The equation from Jacobs and Herendeen (2004) provided the most inaccurate estimation, with an underestimation of 182 mm, while the global equation of Peppe et al. (2018) was the most accurate, only 64 mm higher than the real MAP. The reconstruction of the proportion of precipitation during rainy months (95.5%) was similar to the real modern proportion (96%) (Table 6).

4.3.2. Paleolagoa Seca

Considering the Late Pleistocene age of the fossil flora and its location within the same ecological region than the Panga Forest, we can assume a similar behavior for the pE-MAT relationship in both floras. Therefore, to estimate MAT from the Paleolagoa Seca macroflora, we used the six equations that provided accurate estimations for the Panga Forest LMAT and disregarded the other four equations that resulted in overestimated LMATs.

The LMATs for Paleolagoa Seca ranged between 22.6 and 26.3 °C (Table 7), and MAP reconstructions ranged between 647 and 948 mm (Table 7). The modern MAT of Catalão is 22.6 °C (average of the mean annual temperatures for the 1961–2019 period, data from INMET) and modern MAP is 1434 mm (average of MAPs for the 1961–2019 period, data from INMET). The LMA and LAA results for the Paleolagoa Seca fossil level thus indicate a climate with similar or slightly higher (1 to 3.5 °C) MAT and significantly lower MAP. The highest estimation of MAP (948 mm) is still almost 500 mm lower than modern MAP, pointing to a considerably drier climate. In modern climate, 95.3% of rainfall at Catalão is concentrated in the wettest months, which reflects the markedly seasonal modern climate, in which summer concentrates almost all of the annual precipitation. The results for Paleolagoa Seca Wet-m-P suggest that a relatively lower part of rainfall (87%) occurred during the rainy season. This indicate that the drier climate observed at Paleolagoa Seca was, at a greater extent, due to a decrease in summer precipitation, i.e. to the weakening of the summer monsoon.

Table 3
Radiocarbon dates of the C-LS1 core from Paleolagoa Seca. Ages were calibrated using SHCal13 (Hogg et al., 2013).

Lab Code	Sample Code	Depth (m)	^{14}C yr BP	$\delta^{13}C_{org}$ (‰)	Calibrated age range (cal yr BP) 2σ
Beta - 556,165	C-LS1-25.9	25.90	30,880 ± 160	−22.2	34,400–35,096
Beta - 489,233	C-LS1-26.4	26.40	39,140 ± 380	−25.1	42,376–43,575
Beta - 556,164	C-LS1-27.3	27.30	>43,500 BP	−24.5	–

Table 4
Mineralogical association of Paleolagoa Seca core and outcrop. The fossiliferous level is highlighted in bold.

Core – CLS1		Outcrop - O-LS1		Rock type
		O-LS1-Sam01	quartz, kaolinite, goyazite, crandallite	Grey argillite
C-LS1–26.4	**quartz, anatase, kaolinite, dolomite, dawsonite, crandallite/plumbogommite group**	**O-LS1-Sam02**	**quartz, kaolinite, crandallite, anatase, jarosite**	**Grey argillite with fossils**
C-LS1–27.3	anatase, quartz, kaolinite, hematite, titatomagnetite, dawsonite, crandallite/plumbogommite group	O-LS1-Sam03	quartz, kaolinite, goyazite	Black argillite
		O-LS1-Sam04	quartz, kaolinite, goyazite, crandallite, gypsum	Black argillite
		O-LS1-Sam05	quartz, kaolinite, goyazite, crandallite	Black argillite
C-LS1–28	quartz, anatase, kaolinite, hematite, magnetite, dolomite, dawsonite, pyrite	O-LS1-Sam06	quartz, kaolinite, goyazite, ilmenite	Argillite with argillite clasts
C-LS1–32	quartz, anatase, kaolinite, magnetite, vivianite, dolomite, dawsonite			Argillite with argillite clasts
C-LS1–37	quartz, kaolinite, analcime, dawsonite, anatase			Orto-conglomerate

4.3.3. Paleolago Cemitério

The paleoclimate reconstructions for the Paleolago Cemitério are based on the data presented by Silva (2013) who described the macrofloras of three fossiliferous levels of the Cemitério sequence. We applied the same equations used for Paleolagoa Seca to the data provided by Silva (2013) (Supplementary Materials, Table S1).

Dates for the three fossiliferous levels are from Machado et al. (2014) who documented a radiocarbon age of 51.780 ± 400 yr BP from a fern frond at the older fossiliferous level (FL1) and a radiocarbon age of 48.333 ± 400 yr BP from an angiosperm leaf at the second level (FL2); and from Machado et al. (2013) who estimated the age of the third level (FL3) between 29,700 and 31,500 yr BP based on thermoluminescence and optically stimulated luminescence dates.

The results for FL1 indicated a MAT (20.3 to 23.7 °C) similar to the modern MAT of Catalão and a MAP between 1072 and 1304 mm, lower than modern but higher than the one estimated for the Paleolagoa Seca. The results for FL2 indicated slightly lower but close to modern MAT (19.9 to 23.2 °C) and similar to modern MAP (1240–1480 mm). Results for FL3 documented the lowest MAT estimations (19.2 to 22.7 °C), but still in the range of modern MAT, and a lower than present MAP (1140 to 1364 mm).

5. Discussion

5.1. The Paleolagoa Seca record

The bottom layer of the O-LS1sedimentary sequence, composed of argillite with argillite clasts, is indicative of a deposition under a high-energy flux. The presence of argillite clasts indicates that frequent rains eroded previously deposited sediments and re-deposited them in a lacustrine environment. Diatomite layers interbedded with this argillite layer documented in the C-LS1 indicate periodic deposition of diatom blooms. The transition into a low-energy environment is documented by the black argillite layer visible in both O-LS1 and C-LS1. This dark organic layer indicates deposition in a low-oxygen environment possibly related to the formation of a deeper and stratified lake, prior to 43,500 cal yr BP.

Upward, the fossiliferous level is interpreted to represent a shallower temporary lake, subject to periodic drying, at around 43,000 cal yr BP. The preservation of carbonized fossil leaves indicates deposition in a low-energy and low-oxygen environment, with abundant sediment input and rapid burial. The presence of jarosite in this layer is significant; this iron hydrosulphate often occurs by the oxidation of sulfide minerals, especially pyrite (Cogram, 2018). Its presence could thus indicate that the low-oxygen environment in which the leaves were deposited was exposed to the surface during or shortly after the deposition of this layer. The preservation of the leaves could have been favored by in-lake precipitation of carbonates (dawsonite) that cemented the sediments prior to the subaerial exposure and protected the leaves from rapid decomposition. Dawsonite is the only mineral component detected in the Paleolagoa Seca sequence that is not present in the surrounding rocks and soils of the Catalão complex and thus its presence is likely related to authigenic precipitation in an alkaline supersaturated shallow lake.

The hydrated phosphates of the crandallite group, as well as the other more common minerals encountered in the samples, have been described on the supergene profiles of the carbonatite complex (Alcover Neto and de Toledo, 1993; de Toledo, 1999). Crandallite, vivianite and plumbogommite are known as products of the supergene alteration of apatite (Vieillard, 1978), a major component of the ultramafic-alkaline-carbonatitic complex (de Toledo, 1999). Geochemical studies (Vieillard, 1978; Vieillard et al., 1979; Lucas et al., 1980; Flicoteaux and Lucas, 1984) of lateritic profiles developed on phosphate rocks observed a vertical mineralogical zonation with a decrease in alkalis and hydration, increase in the Al + Fe/P ratio and increase in the degree of Fe oxidation from base to top. In the Paleolagoa Seca succession, this

Table 5
Morphotypes described from the Paleolagoa Seca fossils with their respective taxonomic identifications, life-form types and occurrence within the Cerrado biome.

Morpho-type	Laminar Size	Margin Type	Taxonomy	Life-form type	Habitat (Cerrado physiognomy)
M1	Microphyll	Entire	*Ilex* sp. (Aquifoliaceae)	Tree	Riparian forest, dry forest, savanna.
M2	Microphyll	Entire	*Terminalia fagifolia* (Combretaceae)	Tree	Dry forest, Cerradão, Cerrado (*stricto* sensu), grasslands
M3	Nanophyll	Entire	*Calopogonium* cf. *caeruleum* (Fabaceae)	Liana	Gallery forest, Cerradão
M4	Microphyll	Entire	*Machaerium* cf. *acutifolium* (Fabaceae)	Tree	Dry forest
M5	Nanophyll	Entire	*Mimosa* sp. (Fabaceae)	Herb, shrub or tree	Grasslands, savanna
M6	Nanophyll	Entire	*Stryphnodendron* cf. *adstringens* (Fabaceae)	Tree	Savanna, Cerradão
M7	Nanophyll	Entire	*Endlicheria* cf. *paniculata* (Lauraceae)	Tree	Riparian forest
M8	Microphyll	Entire	*Ocotea sp.* (Lauraceae)	Tree	Forest, riparian forest, savanna
M9	Microphyll	Entire	*Eriotheca gracilipes* (Malvaceae)	Tree	Gallery forest, savanna
M10	Notophyll	Entire	Melastomataceae	Tree	Grasslands, savanna, forests
M11	Microphyll	Entire	*Ficus* cf. *obtusifolia* (Moraceae)	Tree	Forests
M12	Microphyll	Entire	*Pseudolmedia* sp. (Moraceae)	Tree	Gallery and riparian forests
M13	Notophyll	Entire	*Virola* cf. *sebifera* (Myristicaceae)	Tree	Gallery forest
M14	Microphyll	Entire	*Eugenia* sp. (Myrtaceae)	Tree or shrub	Savanna, gallery forest, dry forest, grassland
M15	Microphyll	Entire	*Agonandra excelsa* (Opiliaceae)	Tree	Savanna, dry forest, riparian forest
M16	Microphyll	Entire	*Guettarda viburnoides* (Rubiaceae)	Tree	Gallery forest, savanna, savanna woodland,
M17	Microphyll	Toothed	*Symplocos* sp. (Symplocaceae)	Tree	Gallery forest, dry forest
M18	Microphyll	Entire	unidentified	–	–
M19	Microphyll	Entire	unidentified	–	–

vertical zonation of the crandallite group minerals was not observed. Instead, there is a mixture of the alteration-minerals in the sediment layers. In addition, the absence of the band at 3670 cm^{-1} in the IR spectra and of discrete reflections In (110, d = 4.36 Å and 111, d = 4.18 Å) in the range of 20 to 30° 2θ CuKα from the XRD analyzes showed a kaolinite with high structural defect (Brindley and Brown, 1980), typical of pedogenetic origin (Varajão et al., 2001, 2020). This pattern indicates that the source of the lacustrine sediments were the supergene profiles that had been previously developed by the alteration of the Catalão complex rocks.

With respect to the macroflora composition, seven of the identified taxa are exclusive of gallery or dry forests (Table 5), and the others can occur both in forest and savanna formations. Of those, one (M15, *Agonandra* (*A. brasiliensis*)) is documented by Ribeiro and Walter (2008) as a common component of savanna woodlands (Cerradão). Three species related to morphotypes M6, M9 and M14 (respectively, *Styphnodendron obovatum*, *Eriotheca gracilipes* and *Eugenia dysenterica*) are cited as frequent components of open savannas and one morphotype (M5, *Mimosa*) is typical of shrubby grasslands (Ribeiro and Walter, 2008). The macroflora is mainly composed by arboreal taxa, but the pollen spectra showed that herbaceous taxa were abundant. Poaceae and Asteraceae, although frequent in the pollen spectra, were not identified in the macroflora. Their absence may result from a lower preservation potential of their smaller and/or thinner leaves or from their distribution further away from the depositional site. Fossil leaves deposits tend to register plants growing close to the depositional site, whereas pollen grains can be transported over longer distances. The arboreal component of the pollen spectra is consistent with the presence of both gallery forests and arboreal savannas neighboring the paleolake. *Symplocos* and *Trema micrantha* usually occur in gallery forests within the Cerrado biome (Mendonça et al., 2008; Ribeiro and Walter, 2008). *Cupania*, *Chrysophyllum*, *Ilex*, *Myrsine* and the families Myrtaceae and Melastomataceae occur both in the arboreal savanna and in forest formations (Mendonça et al., 2008). The high frequency of Asteraceae and the presence of shrubs such as *Galianthe*, *Sida* and *Sebastiania* indicate that open savannas and/or shrubby grasslands were present.

Combining the macroflora and pollen records, the picture that emerges for the Paleolagoa Seca fossiliferous level indicates the presence of swampy areas and gallery forests restricted to the immediacies of the paleolake, whereas open savannas and shrubby grasslands covered most of the Catalão plateau. Leaf-margin and leaf-area analyses of the macroflora indicate that this landscape was established under a warmer and significantly drier-than-present climate, similar to the one occurring today in the northeastern portion of the Cerrado biome (da Silva et al., 2008, Fig. 1). Both the presence of a shallow temporary lake and of open savannas and shrubby grasslands in the plateau are consistent with these climate conditions.

In the macrofloras of the Paleolago Cemitério, predominance of forest taxa was also observed, with taxa such as *Machaerium* (FL 1, 2 and 3), *Ocotea* (FL 1 and 3), *Virola sebifera* (FL 3), *Agonandra* (FL 1 and 2) and *Cupania* (FL 1, 2 and 3), also present in Paleolagoa Seca. Other taxa common to both paleolakes are the open savanna taxa *Stryphnodendron* (FL 1), *Eriotheca* (FL 1, 2 and 3) and *Eugenia* (FL 1 and 2), and the gallery forest taxa *Pseudolmedia* (FL 1 and 3) and *Guettarda virbunoides* (FL 1, 2 and 3). According to Ribeiro and Walter (2008), eight of the taxa identified in Paleolago Cemitério are typical of transitional zones between Cerrado and Atlantic Forest or Amazonian Savannas, and five are typical of areas susceptible to flooding. The presence of these taxa corroborates the interpretation of a wetter environment for Paleolago Cemitério than the one reconstructed for Paleolagoa Seca.

5.2. Paleoclimate implications

The low MAP (674–948 mm) together with the relatively low percentage of wet-months precipitation in the total MAP reconstructed for the Paleolagoa Seca macroflora suggest a decrease in the summer monsoon (SASM) rainfall in Central Brazil at around 43,000 cal yr BP. Two main modes of past variability of the SASM are acknowledged in the literature. In a larger temporal scale, SASM is known to respond to interhemispheric insolation variability (Cruz et al., 2005; Kutzbach et al., 2008; Deininger et al., 2019). When summer insolation is higher in Southern Hemisphere, the ITCZ migrates southward and SASM is enhanced; the opposite trend is observed when summer insolation is greater in the Northern Hemisphere (northern monsoon systems are then enhanced; Kutzbach et al., 2008). SASM variability driven by insolation occurs in cycles of ~20 kyr and is well documented by the Botuverá Cave speleothem $\delta^{18}O$ record, at the southern limits of the SASM region (Cruz et al., 2005; Deininger et al., 2019). Superimposed to this larger-scale variability, centennial to millennial-scale events of SASM variability have also been documented during the Pleistocene (Deininger et al., 2019; Novello et al., 2017; Stríkis et al., 2015, 2018). Most of these events have been linked to Dansgaard-Oeschger artic events, i.e. Greenland stadial (GS, glacial) and interstadial (GI, warm) events that alternated during the Pleistocene (Dansgaard et al., 1984). Coupling between SASM variability and GS-GI events have been well documented by paleoclimatic records in northwestern (Kanner et al., 2012; Mosblech et al., 2012), Central-Eastern (Stríkis et al., 2018) and western (Novello et al., 2017) South America. During Greenland stadials, the southward migration of the ITCZ enhances the SASM system, whereas the opposite trend, i.e. weakening of the SASM, is observed

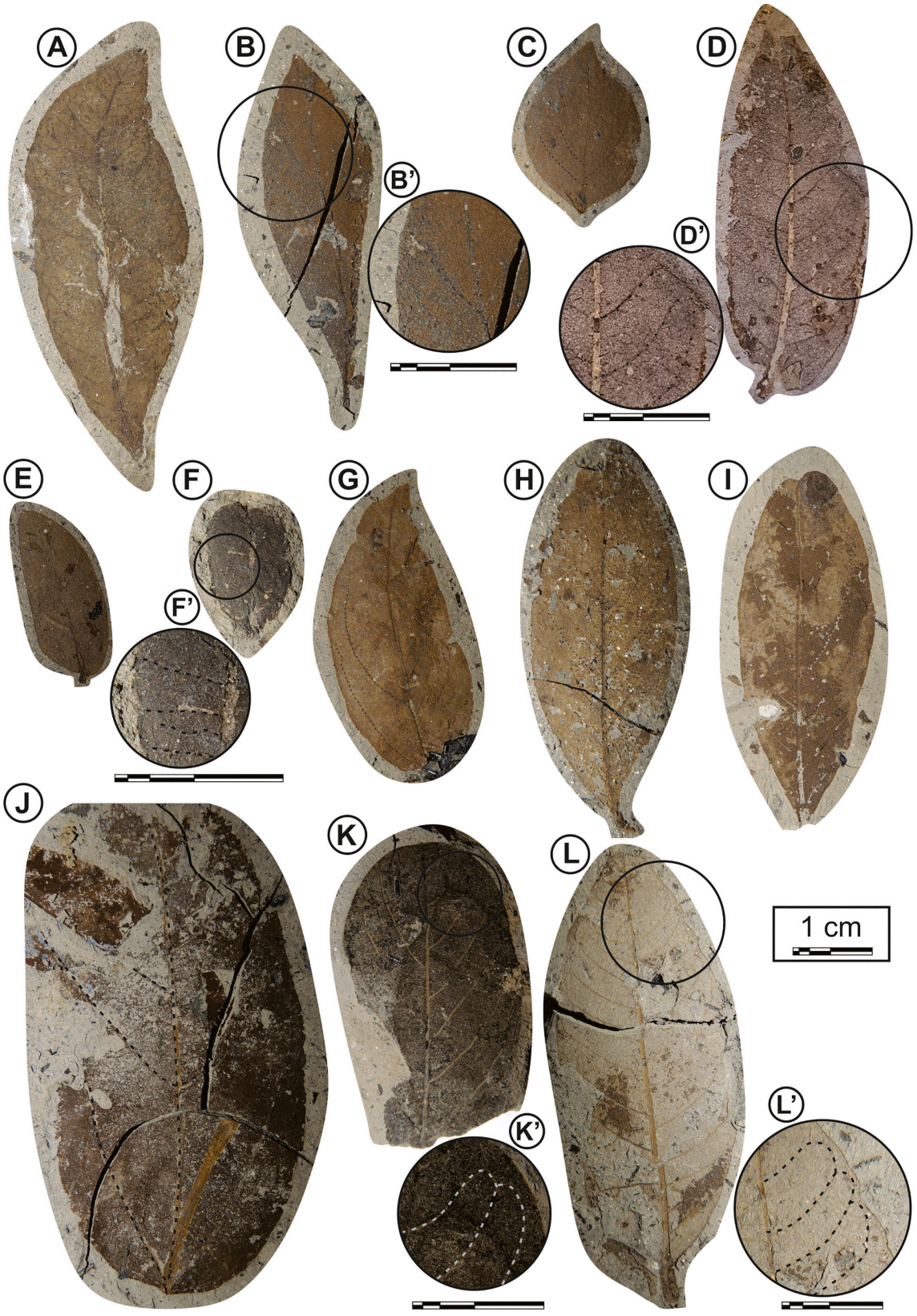

Fig. 3. Morphotypes from the Paleolagoa Seca. A) M1 - Ilex sp. (Aquifoliaceae); B) M2 – Terminalia fagifolia. (Combretaceae); C) M3 - *Calopogonium* cf. *caeruleum* (Fabaceae); D) M4 - Machaerium cf. acutifolium (Fabaceae); E) M5 - Mimosa sp. (Fabaceae); F) M6 - *Stryphnodendron* cf. *adstringens* (Fabaceae); G) M7 - Endlicheria cf. paniculata (Lauraceae); H) M8 - Ocotea sp. (Lauraceae); I) M9 - Eriotheca gracilipes (Malvaceae); J) M10 – Melastomataceae; K) M11 - *Ficus* cf. *obtusifolia* (Moraceae); L) M12 - Pseudolmedia sp. (Moraceae). M) M13 - *Virola* cf. *sebifera* (Myristicaceae); N) M14 - Eugenia sp. (Myrtaceae); O) M15 - Agonandra excelsa (Opiliaceae); P) M16 – Guettarda viburnoides (Rubiaceae); Q) M17 - Symplocos sp. (Symplocaceae); R) M18 - unidentified; S) M19 - unidentified; T) *Pteridium arachnoideum*.

Fig. 3. (*continued*).

during Greenland Interstadials. The deposition of the Paleolagoa Seca fossiliferous level took place during the Greenland Interstadial event 11 (GI-11, Fig. 5) (as defined by Rasmussen et al., 2014), which is consistent with our results showing a significant lower monsoon precipitation in central Brazil. A dry event during GI-11 is also documented in speleothem $\delta^{18}O$ records from Central-Eastern and Northeastern Brazil (respectively Sem Fim/Grande and Marota caves (Stríkis et al., 2018; Fig. 5).

The Paleolago Cemitério FL2 was deposited during Greenland Stadial GS-13 (Fig. 5), that also correspond to a Heinrich event - i.e. North Atlantic cold episode associated with massive deposition of ice-rafted detritus (Hemming, 2004). The speleothem $\delta^{18}O$ records from Central-Eastern and Northeastern Brazil document a strengthening of the SASM during this event, which is consistent with the higher MAP reconstructed for FL2. The similar to present proportion of wet-months precipitation reconstructed for this macroflora (94%) is also consistent with a predominantly monsoon derived annual precipitation. Our results document a MAP for the Paleolagoa Seca around 35% lower than

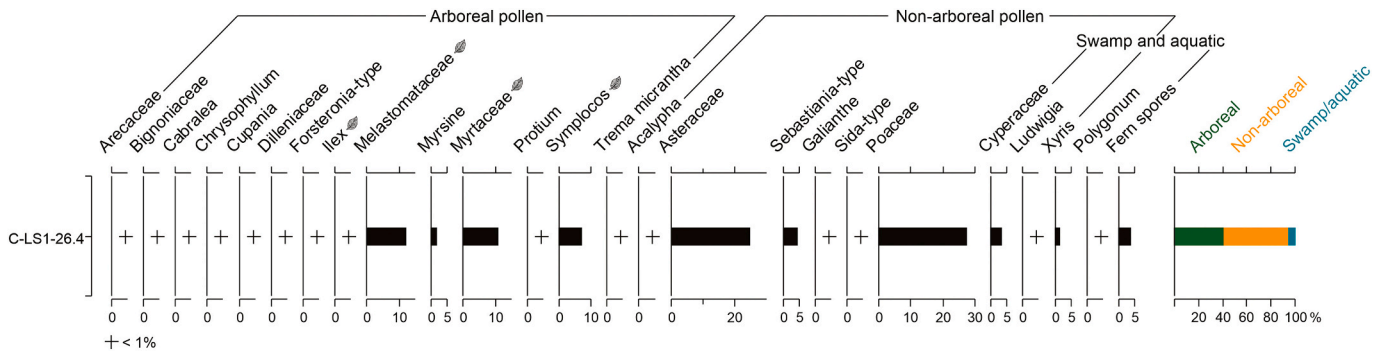

Fig. 4. Pollen percentage diagram for the Paleolagoa Seca fossiliferous level. Leaf symbols indicate taxa that were also present in the macroflora.

Table 6
MAT and MAP results for the Riparian forest of the Panga Ecological Station.

Riparian forest of the Panga Ecological Station			
LMA (pE = 0.89)			
Actual MAT: 22 °C			
Model	Reference	***LMAT*** (°C)	***σ*[*LMAT*]**
North, Central, South America	Wilf (1997)	27.7	1,2
South America	Gregory-Wodzicki (2000)	28.1	1,3
Tropical South America	Kowalski (2002)	**24.0**	**1,6**
South America (isotherm)	Aizen and Ezcurra (2008)	**23.1**	**1,6**
South America (cell)	Aizen and Ezcurra (2008)	26.3	1,7
South America	Hinojosa et al. (2011)	**24.5**	**1,1**
South America	Kennedy et al. (2014)	30.8	1,8
Southern Hemisphere	Kennedy et al. (2014)	**21.0**	**1,1**
Oceania, Japan, North America, South America, Southern Africa	Kennedy et al. (2014)	**21.8**	**0,8**
Global	Peppe et al. (2018)	**23.2**	**0,8**

LAA		
Actual MAP: 1456 mm; Actual Wet-m-P: 1398 mm (96% of MAP)		
Model	Reference	MAP (mm)
North and South America and Africa	Wilf et al. (1998)	1366 (−90)
Tropical Africa and Bolivia	Jacobs and Herendeen (2004)	1350 (−106) Wet-m-*P* = 1276 (95,5% of MAP)
North and South America and Africa	Jacobs and Herendeen (2004)	1274 (−182)
Global	Peppe et al. (2018)	1520 (+64)

Bold numbers indicate accurate LMAT predictions.

Table 7
MAT and MAP results for the fossiliferous level of Paleolagoa Seca.

Paleolagoa Seca macroflora			
LMA – pE = 0.95			
Model	Reference	***LMAT*** (°C)	***σ*[*LMAT*]**
Tropical South America	Kowalski (2002)	26.3	2.0
South America (isotherm)	Aizen and Ezcurra (2008)	25.4	2.0
South America	Hinojosa et al. (2011)	26.0	1.3
Southern Hemisphere	Kennedy et al. (2014)	22.6	1.3
Oceania, Japan, North America, South America, Southern Africa	Kennedy et al. (2014)	23.0	1.0
Global	Peppe et al. (2018)	24.3	1.0

LAA – MlnA = 6.2		
Model	Reference	MAP (mm)
North and South America and Africa	Wilf et al. (1998)	647
Tropical Africa and Bolivia	Jacobs and Herendeen (2004)	886 Wet-m-*P* = 773 (87% of MAP)
North and South America and Africa	Jacobs and Herendeen (2004)	786
Global	Peppe et al. (2018)	948

the Paleolago Cemitério FL2, providing an order of magnitude for the rainfall variability related to GS-GI cycles in central Brazil.

The MATs reconstructed for the Paleolagoa Seca are similar or higher than present, which indicates warm temperatures during GI-11 in central Brazil. Summer insolation at around 43,000 cal yr BP was close to modern values at the Paleolagoa Seca latitude (Fig. 5) and since insolation is one of the main controlling factors of surface temperature, it is consistent with warm, similar-to-present, temperatures. In addition to high summer insolation, the effect of low precipitation might also have played a role in increasing MAT. Trenberth and Shea (2005) discussed the co-variability of precipitation and surface temperature during the last decades and showed that less summer precipitation is correlated with higher continental temperatures. According to those authors, less precipitation and reduced soil moisture cause a decrease in evaporation that results in an increase in the ratio of sensible to latent heat fluxes and in a consequent rise in land temperature. At the Paleolagoa Seca, similar-to-present summer insolation combined with the lower-than-present summer precipitation could thus have resulted in a warm climate as detected by the reconstructed MAT. However, an overestimation of the reconstructed MAT cannot be ruled out because leaf margin is also influenced by water availability. The presence of leaf teeth is related to enhanced sap flow and hence to increased water loss (Peppe et al., 2018); consequently, entire-margined species predominate in locally dry environments. At the Paleolagoa Seca, there is a mixture of gallery forest and dry forest/savanna species and the contribution of low water availability to the lack of toothed species must also be considered. On the other hand, the absence of cold-adapted taxa such as *Araucaria* and *Drymis* in both pollen and macroflora records is consistent with warm temperatures.

6. Conclusions

The Paleolagoa Seca fossil macroflora and its mineralogical association indicate around 43,000 cal yr BP the presence of a shallow lake subject to temporary drying, with in-lake carbonate precipitation that

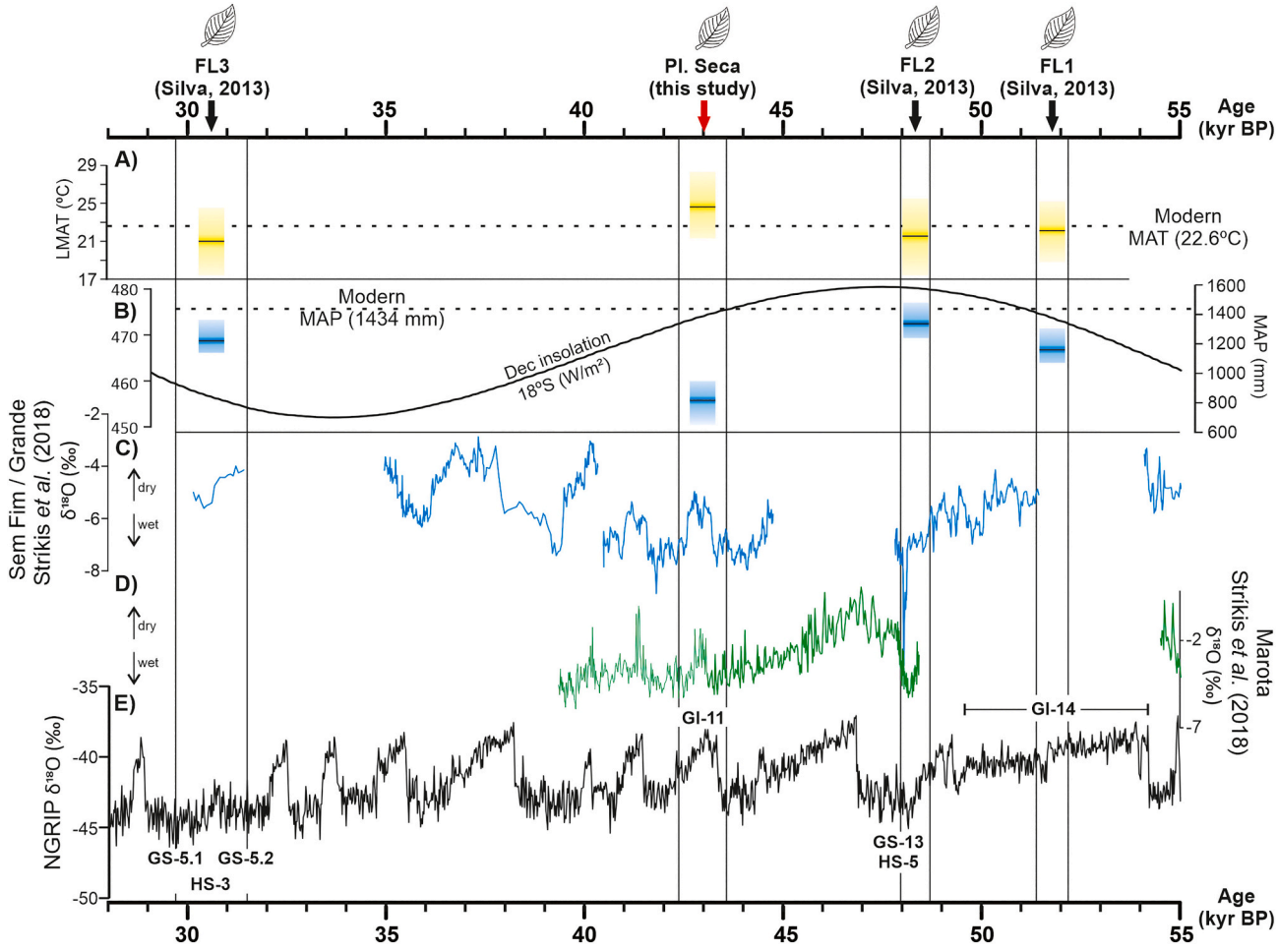

Fig. 5. Comparison between the Mean Annual Temperature and Mean Annual Precipitation reconstructed for the paleolakes Seca and Cemitério with other paleoclimatic records. A) Reconstructed MATs for the four macrofloras; B) Reconstructed MAPs for the four macrofloras and austral summer insolation (December) curve for Paleolagoa Seca latitude (from Laskar et al., 2004); C) Central-eastern $\delta^{18}O$ speleothem records from Stríkis et al. (2018); D) North-eastern $\delta^{18}O$ speleothem records from Stríkis et al. (2018); E) NGRIP ice core $\delta^{18}O$ record showing GS and GI intervals.

probably enabled leaf preservation. The shallowing of the lake is related to a low mean annual precipitation, which is linked to the weakening of SASM. The macroflora and pollen record composition document the presence of gallery forests, dry forests and open savanna physiognomies, such as *Cerrado stricto* sensu. The Paleolagoa Seca macroflora was deposited during a Greenland Interstadial episode (GI-11), during which speleothem records from Central-eastern Brazil also document a weakening of the SASM, associated to the northward displacement of the ITCZ. Our study indicates that during GI-11, the annual precipitation at the Paleolagoa Seca site was at least 500 mm lower than present and the climate was warm, with a mean annual temperature similar or slightly higher than present.

Supplementary data to this article can be found online at https://doi.org/10.1016/j.palaeo.2021.110243.

Declaration of Competing Interest

The authors declare that they have no known competing financial interests or personal relationships that could have appeared to influence the work reported in this paper.

Acknowledgments

The first author thanks CAPEs for the doctoral scholarship (Finance Code 001) and the authors thank CNPq (grant 306424/2016-9 to AFDCV) and FAPEMIG (grant PPM 00326-18 to AFDCV and other grants to JSB and Karin Meyer) for financial support.

References

Aizen, M., Ezcurra, C., 2008. Do leaf margins of the temperate forest flora of Southern South America reflect a warmer past? Glob. Ecol. Biogeogr. 17, 164–174. https://doi.org/10.1111/j.1466-8238.2007.00350.x.

Alcover Neto, A., de Toledo, M.C.M., 1993. Evolução supérgena do carbonatito de Juquiá (SP). Revista do Instituto Geológico 14, 31–43. https://doi.org/10.5935/0100-929X.19930003.

Alvares, C.A., Stape, J.L., Sentelhas, P.C., de Moraes Gonçalves, J.L., Sparovek, G., 2013. Köppen's climate classification map for Brazil. metz 22, 711–728. https://doi.org/10.1127/0941-2948/2013/0507.

Ash, A., Ellis, B., Hickey, L., Johnson, K., Wilf, P., Wing, S., 1999. Manual of Leaf Architecture: Morphological Description of Dicotyledonous and Net-Veined Monocotyledonous Angiosperms. Smithsonian Institution, Washington, DC (Privately published and distributed).

Brindley, G.W., Brown, G. (Eds.), 1980. Crystal Structures of Clay Minerals and their X-Ray Identification, new ed. Monograph/Mineralogical Society. Mineralogical Society, London.

Brotto, M., Cervi, A., Santos, E., 2013. The genus Ocotea (Lauraceae) in Parana State, Brazil. Rodriguésia 64, 495–525. https://doi.org/10.1590/S2175-78602013000300004.

Ferreira, F.S.O., Cardoso, E., 2013. Estrutura fitossociológia de Campo Sujo no município de Catalão - GO. Caminhos de Geografia 14 (45), 110–119.

Cardoso, N., Iannuzzi, R., 2006. Pteridium catalensis sp. nov., uma nova pteridófita fóssil do complexo carbonatítico Catalão I, Goiás. RBP 9, 303–310. https://doi.org/10.4072/rbp.2006.3.05.

Cogram, P., 2018. Jarosite. In: Reference Module in Earth Systems and Environmental Sciences. Elsevier. https://doi.org/10.1016/B978-0-12-409548-9.10960-1.

Cruz, F.W., Burns, S.J., Karmann, I., Sharp, W.D., Vuille, M., Cardoso, A.O., Ferrari, J.A., Silva Dias, P.L., Viana, O., 2005. Insolation-driven changes in atmospheric circulation over the past 116,000 years in subtropical Brazil. Nature 434, 63–66. https://doi.org/10.1038/nature03365.

Dansgaard, W., Johnsen, S.J., Clausen, H.B., Dahl-Jensen, D., Gundestrup, N., Hammer, C.U., Oeschger, H., 1984. North Atlantic climatic oscillations revealed by deep greenland ice cores. In: Climate Processes and Climate Sensitivity. American Geophysical Union (AGU), pp. 288–298. https://doi.org/10.1029/GM029p0288.

Deininger, M., Ward, B.M., Novello, V.F., Cruz, F.W., 2019. Late quaternary variations in the South American monsoon system as inferred by Speleothems—new perspectives using the SISAL database. Quaternary 2, 6. https://doi.org/10.3390/quat2010006.

Dutra, S.M., Salimena, F.R.G., Menini Neto, L., 2012. Annonaceae na Serra Negra, Minas Gerais, Brasil. Rodriguésia 63, 785–793. https://doi.org/10.1590/S2175-78602012000400004.

Ellis, B., Daly, D.C., Hickey, L.J., 2009. Manual of Leaf Architecture. Cornell University Press, Ithaca.

Faegri, K., Iversen, J., 1989. Textbook of Pollen Analysis (4th edn by Faegri, K., Kaland, PE & Krzywinski, K.).

Farmer, V.C. (Ed.), 1974. The Infrared Spectra of Minerals. Mineralogical Society, London.

Feldman, R.M., Chapman, R.E., Hannibal, J.T., Paleontological Society, 1989. Paleotechniques. Paleontological Society, S.l.

Ferreira, C.S., Moreno, M.I.C., 2010. Levantamento fitossociológico e estrutura populacional em remanescente de vegetação nativa de cerrado na área urbana de Catalão, Goiás. In: VII congresso de Ensino, Pesquisa e Extensão/CONPEEX 2010, 2010, Goiânia.

Fick, S.E., Hijmans, R.J., 2017. WorldClim 2: new 1-km spatial resolution climate surfaces for global land areas. Int. J. Climatol. 37, 4302–4315. https://doi.org/10.1002/joc.5086.

Flicoteaux, R., Lucas, J., 1984. Weathering of phosphate minerals. In: Nriagu, J.O., Moore, P.B. (Eds.), Phosphate Minerals. Springer, Berlin, Heidelberg, pp. 292–317. https://doi.org/10.1007/978-3-642-61736-2_9.

Gregory-Wodzicki, K.M., 2000. Relationships between leaf morphology and climate, Bolivia: implications for estimating paleoclimate from fossil floras. Paleobiology 26, 668–688. https://doi.org/10.1666/0094-8373(2000)026<0668:RBLMAC>2.0.CO;2.

Hemming, S., 2004. Heinrich events: massive late Pleistocene detritus layers of the North Atlantic and their global cli. Rev. Geophys. 42.

Hinojosa, L.F., Pérez, F., Gaxiola, A., Sandoval, I., 2011. Historical and phylogenetic constraints on the incidence of entire leaf margins: insights from a new South American model. Glob. Ecol. Biogeogr. 20, 380–390. https://doi.org/10.1111/j.1466-8238.2010.00595.x.

Hogg, A.G., Hua, Q., Blackwell, P.G., Niu, M., Buck, C.E., Guilderson, T.P., Heaton, T.J., Palmer, J.G., Reimer, P.J., Reimer, R.W., Turney, C.S.M., Zimmerman, S.R.H., 2013. SHCal13 southern hemisphere calibration, 0–50,000 years cal BP. Radiocarbon 55, 1889–1903. https://doi.org/10.2458/azu_js_rc.55.16783.

IBGE (Ed.), 2004. Vocabulário básico de recursos naturais e meio ambiente, 2a. ed. IBGE, Rio de Janeiro. I.B. de G. e E. (Ed.).

Jacobs, B.F., 1999. Estimation of rainfall variables from leaf characters in tropical Africa. Palaeogeogr. Palaeoclimatol. Palaeoecol. 145, 231–250. https://doi.org/10.1016/S0031-0182(98)00102-3.

Jacobs, B., Herendeen, P., 2004. Eocene dry climate and woodland vegetation in tropical Africa reconstructed from fossil leaves from northern Tanzania. Palaeogeogr. Palaeoclimatol. Palaeoecol. 213, 115–123. https://doi.org/10.1016/j.palaeo.2004.07.007.

Kanner, L.C., Burns, S.J., Cheng, H., Edwards, R.L., 2012. High-Latitude Forcing of the South American Summer Monsoon during the last Glacial. Science 335, 570–573. https://doi.org/10.1126/science.1213397.

Kennedy, E.M., Arens, N.C., Reichgelt, T., Spicer, R.A., Spicer, T.E.V., Stranks, L., Yang, J., 2014. Deriving temperature estimates from Southern Hemisphere leaves. Palaeogeogr. Palaeoclimatol. Palaeoecol. 412, 80–90. https://doi.org/10.1016/j.palaeo.2014.07.015.

Kowalski, E.A., 2002. Mean annual temperature estimation based on leaf morphology: a test from tropical, in: South America. Palaeogeogr. Palaeoclimatol. Palaeoecol. 188, 141–165.

Laskar, J., Robutel, P., Joutel, F., Gastineau, M., Correia, A.C.M., Levrard, B., 2004. A long-term numerical solution for the insolation quantities of the Earth. Astron. Astrophys. 428, 261–285. https://doi.org/10.1051/0004-6361:20041335.

Kutzbach, J.E., Liu, X., Liu, Z., Chen, G., 2008. Simulation of the evolutionary response of global summer monsoons to orbital forcing over the past 280,000 years. Clim. Dyn. 30, 567–579. https://doi.org/10.1007/s00382-007-0308-z.

Lopes, S.de.F., Schiavini, I., 2007. Dinâmica da comunidade arbórea de mata de galeria da Estação Ecológica do Panga, Minas Gerais, Brasil. Acta Bot. Bras. 21, 249–261. https://doi.org/10.1590/S0102-33062007000200001.

Lucas, J., Flicoteaux, R., Nathan, Y., Prévôt, L., Shahar, Y., 1980. Different Aspects of Phosphorite Weathering.

Machado, V.de.S., Volkmer-Ribeiro, C., Iannuzzi, R., 2014. Late Pleistocene climatic changes in central Brazil indicated by freshwater sponges. Int. J. Geosci. 5, 799–815. https://doi.org/10.4236/ijg.2014.58071.

Machado, V.de.S., Volkmer-Ribeiro, C., Iannuzzi, R., 2013. First record of preserved gemmules of a Pleistocene assemblage of freshwater sponges. Rev. Bras. Paleontol. https://doi.org/10.4072/rbp.2013.2.01.

Margalho, L.F., 2009. Rubiaceae Juss. da Restinga da APA de Algodoal/Maiandeua, Maracanã, Pará, Brasil Rubiaceae Juss. Of the Restinga from APA of Algodoal/Maiandeua, Maracanã, Pará, Brazil, 4, p. 38.

Martins, E.G.A., Pirani, J.R., 2010. Flora da Serra do Cipó, Minas Gerais: Moraceae. Boletim de Botânica 28, 69–86. https://doi.org/10.11606/issn.2316-9052.v28i1p69-86.

de Mattos, C.M.J., da Silva e Silva, W.L., de Carvalho, C.S., Lima, A.N., de Faria, S.M., de Lima, H.C., 2018. Flora das cangas da serra dos Carajás, Pará, Brasil: Leguminosae. Rodriguésia 69, 1147–1220. https://doi.org/10.1590/2175-7860201869323.

Mendonça, R.C., Felfili, J.M., Walter, B., Silva Jr., M., Rezende, A., Filgueiras, T.S., Nogueira, P.E., Fagg, C., 2008. Flora vascular do bioma Cerrado: Checklist com 12.356 espécies, 2, pp. 421–1279.

Miller, I., Brandon, M., Hickey, L., 2006. Using leaf margin analysis to estimate the mid-cretaceous (Albian) paleolatitude of the Baja BC block. Earth Planet. Sci. Lett. 245, 95–114. https://doi.org/10.1016/j.epsl.2006.02.022.

Mosblech, N., Bush, M., Gosling, W., Thomas, L., Calsteren, P., Correa-Metrio, A., Valencia, B., Curtis, J., Van Woesik, R., 2012. North Atlantic forcing of Amazonian precipitation during the last ice age. Nat. Geosci. https://doi.org/10.1038/ngeo1588.

Novello, V.F., Cruz, F.W., Vuille, M., Stríkis, N.M., Edwards, R.L., Cheng, H., Emerick, S., de Paula, M.S., Li, X., de S. Barreto, E., Karmann, I., Santos, R.V., 2017. A high-resolution history of the South American Monsoon from last Glacial Maximum to the Holocene. Sci. Rep. 7, 1–8. https://doi.org/10.1038/srep44267.

Oliveira Filho, A., Ratter, J.A., 2002. Vegetation Physiognomies and Woody Flora of the Cerrado Biome. ResearchGate. https://www.researchgate.net/publication/312975423_Vegetation_physiognomies_and_woody_flora_of_the_Cerrado_Biome (accessed 7.12.20).

de Oliveira, M.I.U., Funch, L.S., de A.R. dos Santos, F., Landrum, L.R., 2011. Aplicação de caracteres morfoanatômicos foliares na taxonomia de Campomanesia Ruiz & Pavón (Myrtaceae). Acta Bot. Bras. 25, 455–465. https://doi.org/10.1590/S0102-33062011000200021.

Peppe, D.J., Baumgartner, A., Flynn, A., Blonder, B., 2018. Reconstructing paleoclimate and paleoecology using fossil leaves. In: Croft, D.A., Su, D.F., Simpson, S.W. (Eds.), Methods in Paleoecology: Reconstructing Cenozoic Terrestrial Environments and Ecological Communities, Vertebrate Paleobiology and Paleoanthropology. Springer International Publishing, Cham, pp. 289–317. https://doi.org/10.1007/978-3-319-94265-0_13.

Rasmussen, S.O., Bigler, M., Blockley, S.P., Blunier, T., Buchardt, S.L., Clausen, H.B., Cvijanovic, I., Dahl-Jensen, D., Johnsen, S.J., Fischer, H., Gkinis, V., Guillevic, M., Hoek, W.Z., Lowe, J.J., Pedro, J.B., Popp, T., Seierstad, I.K., Steffensen, J.P., Svensson, A.M., Vallelonga, P., Vinther, B.M., Walker, M.J.C., Wheatley, J.J., Winstrup, M., 2014. A stratigraphic framework for abrupt climatic changes during the last Glacial period based on three synchronized Greenland ice-core records: refining and extending the INTIMATE event stratigraphy. Quat. Sci. Rev. 106, 14–28. https://doi.org/10.1016/j.quascirev.2014.09.007.

Ribeiro, J., Walter, B., 2008. As principais fitofisionomias do bioma Cerrado, pp. 151–212.

Ribeiro, C.C., Brod, J.A., Petrinovic, I.A., Gaspar, J.C., Brod, T.C.J., 2001. Pipes de brecha e atividade magmática explosiva no Complexo alcalino-carbonatítico de Catalão I, Goiás. Rev. Bras. Geoci. 31, 417–426.

Santos-Silva, J., Fragomeni, S.M., de A. Tozzi, A.M.G., 2015. Revisão taxonômica das espécies de Mimosa ser. Leiocarpae sensu lato (Leguminosae - Mimosoideae). Rodriguésia 66, 95–154. https://doi.org/10.1590/2175-7860201566107.

Schiavini, A.C.M., 1990. Estudio de la relación entre el hombre y los pinnípedos en el proceso adaptativo humano al Canal de Beagle, Tierra del Fuego, Argentina (Tesis Doctoral). Universidad de Buenos Aires. Facultad de Ciencias Exactas y Naturales.

Silva, V.B.S., Kousky, V.E., 2012. The South American monsoon system: climatology and variability. Mod. Climatol. https://doi.org/10.5772/38565.

da Silva, A.S., Rosa, R., 2019. Mapa de capacidade e potencial do uso da terra do município de Catalão (GO). Caderno de Geografia 29, 954–977. https://doi.org/10.5752/P.2318-2962.2019v29n59p954.

da Silva, F., Assad, E., Evangelista, B., 2008. Caracterização climática do bioma Cerrado. Cerrado: ecologia e flora 1, 69–88.

Silva, S.C.S.E., 2013. Flora pleistocênica do Paleolago Cemitério, Catalão, GO: taxonomia e fitofisionomia. PhD Thesis. Instituto de Geociências, Universidade Federal do Rio Grande do Sul (UFRGS).

de Sousa, V.F., de T.M. Ribeiro, R., Loiola, M.I.B., Versieux, L.M., 2018. Combretaceae no estado do Rio Grande do Norte, Brasil. Rodriguésia 69, 1771–1787. https://doi.org/10.1590/2175-7860201869417.

Stríkis, N.M., Chiessi, C.M., Cruz, F.W., Vuille, M., Cheng, H., de S. Barreto, E.A., Mollenhauer, G., Kasten, S., Karmann, I., Edwards, R.L., Bernal, J.P., dos R. Sales, H., 2015. Timing and structure of Mega-SACZ events during Heinrich Stadial 1. Geophys. Res. Lett. 42, 5477–5484A. https://doi.org/10.1002/2015GL064048.

Stríkis, N.M., Cruz, F.W., Barreto, E.A.S., Naughton, F., Vuille, M., Cheng, H., Voelker, A.H.L., Zhang, H., Karmann, I., Edwards, R.L., Auler, A.S., Santos, R.V., Sales, H.R., 2018. South American monsoon response to iceberg discharge in the North Atlantic. PNAS 115, 3788–3793. https://doi.org/10.1073/pnas.1717784115.

de Toledo, M.C.M., 1999. Mineralogia dos principais fosfatos do maciço alcalino-carbonatítico de Catalão I (GO) e sua evolução no perfil laterítico (text). Universidade de São Paulo. https://doi.org/10.11606/T.44.2015.tde-03062015-101248.

Trenberth, K.E., Shea, D.J., 2005. Relationships between precipitation and surface temperature. Geophys. Res. Lett. 32, L14703 https://doi.org/10.1029/2005GL022760.

Varajão, A.F.D.C., Gilkes, R.J., Hart, R.D., 2001. The relationships between kaolinite crystal properties and the origin of materials for a Brazilian kaolin deposit. Clay Clay Miner. 49, 44–59.

Varajão, A.F.D.C., Mateus, A.C.C., Santos, M.C., Varajão, C.A.C., Oliveira, F.S., Yvon, J., 2020. The Cenozoic deposits of the ancient landscapes of Quadrilátero Ferrífero

highlands, Southeastern Brazil: Sedimentation, pedogenesis and landscape evolution. Catena 195. https://doi.org/10.1016/j.catena.2020.104813.
Vieillard, P., 1978. Géochimie des phosphates. Étude thermodynamique. Application à la genèse et à l'altération des apatites, Sciences Géologiques, bulletins et mémoires. Persée - Portail des revues scientifiques en SHS 1, 181.
Vieillard, P., Tardy, Y., Nahon, D., 1979. Stability fields of clays and aluminum phosphates; parageneses in lateritic weathering of argillaceous phosphatic sediments. Am. Mineral. 64, 626–634.
Wilf, P., 1997. When are leaves good thermometers? A new case for leaf margin analysis. Paleobiology 23, 373–390.
Wilf, P., Wing, S.L., Greenwood, D.R., Greenwood, C.L., 1998. Using fossil leaves as paleoprecipitation indicators: an Eocene example. GEOLOGY 26, 203–206. https://doi.org/10.1130/0091-7613(1998)026<0203:UFLAPI>2.3.CO;2.
Wolfe, J.A., 1995. Paleoclimatic estimates from tertiary leaf assemblages. Annu. Rev. Earth Planet. Sci. 23, 119–142.